

First principles study of hafnium intercalation between graphene and Ir(111) substrate

Hao Peng(彭浩), Xin Jin(金鑫), Yang Song(宋洋), and Shixuan Du(杜世萱)

Citation: Chin. Phys. B, 2022, 31 (**10**): 106801. DOI: 10.1088/1674-1056/ac6941
Journal homepage: http://cpb.iphy.ac.cn; http://iopscience.iop.org/cpb

What follows is a list of articles you may be interested in

C_9N_4 as excellent dual electrocatalyst: A first principles study

Wei Xu(许伟), WenWu Xu(许文武), and Xiangmei Duan(段香梅)
Chin. Phys. B, 2021, 30 (**9**): 096802. DOI: 10.1088/1674-1056/ac0ccf

First principles study of behavior of helium at Fe(110)-graphene interface

Yan-Mei Jing(荆艳梅) and Shao-Song Huang(黄绍松)
Chin. Phys. B, 2021, 30 (**4**): 046802. DOI: 10.1088/1674-1056/abd46d

Interaction of two symmetric monovacancy defects in graphene

Wen-Yan Xu(徐文焱), Li-Zhi Zhang(张礼智), Li Huang(黄立), Yan-De Que(阙炎德), Ye-Liang Wang(王业亮), Xiao Lin(林晓), Shi-Xuan Du(杜世萱)
Chin. Phys. B, 2019, 28 (**4**): 046801. DOI: 10.1088/1674-1056/28/4/046801

Fabrication and properties of silicene and silicene–graphene layered structures on Ir (111)

Meng Lei, Wang Ye-Liang, Zhang Li-Zhi, Du Shi-Xuan, Gao Hong-Jun
Chin. Phys. B, 2015, 24 (**8**): 086803. DOI: 10.1088/1674-1056/24/8/086803

Intercalation of metals and silicon at the interface of epitaxial graphene and its substrates

Huang Li, Xu Wen-Yan, Que Yan-De, Mao Jin-Hai, Meng Lei, Pan Li-Da, Li Geng, Wang Ye-Liang, Du Shi-Xuan, Liu Yun-Qi, Gao Hong-Jun
Chin. Phys. B, 2013, 22 (**9**): 096803. DOI: 10.1088/1674-1056/22/09/096803

First principles study of hafnium intercalation between graphene and Ir(111) substrate

Hao Peng(彭浩)[1], Xin Jin(金鑫)[1], Yang Song(宋洋)[1], and Shixuan Du(杜世萱)[1,2,3,4,†]

[1] *Institute of Physics, and University of Chinese Academy of Sciences, Chinese Academy of Sciences, Beijing* 100190, *China*
[2] *CAS Center for Excellence in Topological Quantum Computation, University of Chinese Academy of Sciences, Beijing* 100190, *China*
[3] *Beijing National Center for Condensed Matter Physics, Beijing* 100190, *China*
[4] *Songshan Lake Materials Laboratory, Dongguan* 523808, *China*

(Received 25 February 2022; revised manuscript received 7 April 2022; accepted manuscript online 22 April 2022)

The intercalation of heteroatoms between graphene and metal substrates is a promising method for integrating epitaxial graphene with functional materials. Various elements and their oxides have been successfully intercalated into graphene/metal interfaces to form graphene-based heterostructures, showing potential applications in electronic devices. Here we theoretically investigate the hafnium intercalation between graphene and Ir(111). It is found that the penetration barrier of Hf atom is significantly large due to its large atomic radius, which suggests that hafnium intercalation should be carried out with low deposition doses of Hf atoms and high annealing temperatures. Our results show the different intercalation behaviors of a large-size atom and provide guidance for the integration of graphene and hafnium oxide in device applications.

Keywords: first principles calculation, intercalation, graphene, hafnium

PACS: 68.43.Bc, 81.05.ue, 68.35.Fx **DOI:** 10.1088/1674-1056/ac6941

1. Introduction

Graphene, an atomically thin two-dimensional (2D) material with excellent mechanical properties and unique electronic and optical properties, shows broad applications in a variety of functional devices.[1–3] One of the methods to get high-quality and single-crystalline graphene is the epitaxial growth on transition metal substrates.[4–9] However, the electronic structures of graphene obtained in such a way are usually distorted, hindering the applications of graphene.[10–12] One effective approach for this problem is intercalating heteroatoms into graphene/metal interfaces, which not only weakens the interaction between graphene and metal substrates,[13–19] but also provides the feasibility for the integration of graphene and other 2D materials without transfer process, whereby functional devices with clean interface can be achieved.[20,21] Recently, several studies reported the oxides intercalation between graphene and metal substrates, such as SiO_2,[22,23] GeO_x,[24] and MgO.[25] The oxides intercalation was achieved through the stepwise intercalation of heteroatoms and oxygen. After that, *in situ* graphene devices could be fabricated, and the transport properties of epitaxial graphene could be measured and explored.

Due to the higher dielectric constant, HfO_2 can exhibit better performance in electronic devices compared to SiO_2, GeO_x, and MgO,[26] making the HfO_2 intercalation between graphene and metal substrates highly desired. To realize the HfO_2 intercalation, it is critical to achieve Hf intercalation in graphene/metal systems, since the successful intercalation of Hf as well as the maintenance of sharp interfaces and intact epitaxial graphene, which can be ensured by the intercalation method, are essential for the subsequent oxidation operation. To date, the Hf intercalation has been experimentally achieved in less than onemonolayer epitaxial graphene on Ir(111) substrates.[27] Although the incomplete graphene can facilitate the Hf intercalation through graphene edges or pre-existing defects, it is not suitable for the oxidation operation since it cannot resist the corrosion of oxygen.[28,29] Thus, investigation of Hf intercalation in epitaxial defect-free graphene is still desired. Previously, taking Si intercalation between graphene/Ru as a model, several mechanisms have been proposed to account for heteroatoms' intercalation in epitaxial defect-free graphene.[30,31] However, considering that the atomic radius of Hf atom is significantly larger than that of Si atom, it is unknown whether the scenario of Si atoms applies to Hf atoms.

In this paper, we investigate the Hf intercalation between graphene and Ir(111) substrate using first principle calculations. Based on previously reported mechanism which involves cooperative interaction of heteroatoms and substrates, we sequentially investigate the following processes: the adsorption of Hf atoms on graphene/Ir(111), the formation of carbon vacancies in Hf/graphene/Ir(111), the penetration of Hf adatoms, and the diffusion of intercalated Hf atoms at the interface. We find that during the process, the vacancy formation energies and diffusion barriers are small while the penetration barriers are abnormally large, which is different from the

[†]Corresponding author. E-mail: sxdu@iphy.ac.cn

© 2022 Chinese Physical Society and IOP Publishing Ltd

case where all energies or barriers are small in Si intercalation between graphene/Ru(0001).[30] The high penetration barriers indicate that the general condition usually employed in Si or SiO_2 intercalation experiments are not applicable to the Hf or HfO_2 intercalation. Therefore, we propose a strategy with a low deposition dose of Hf atoms and a high annealing temperature for Hf or HfO_2 intercalation, which would eliminate the effect of the high penetration barriers of Hf atoms.

2. Methods

First principles calculations based on density functional theory (DFT) were performed using Vienna *ab initio* simulation package (VASP).[32,33] The projector augmented wave method[34] was used to describe the electron–ion interaction. For the graphene/Ir(111) and Hf/graphene/Ir(111) system, as suggested in the literature[35–37] and in our test calculations (see Figs. 1 and S1), local density approximation functional was employed, which allows us to obtain similar geometric and electronic structures with two layers of substrate as those using PBE-D3 functional (in which Grimme's empirical correction is used to describe the van der Waals interaction[38]) with three layers of substrate. The energy cutoff of the plane-wave basis sets was 400 eV and a Γ point k-sampling was employed. The periodic slab model of the graphene/Ir(111) system included two layers of 9×9 Ir(111), one layer of 10×10 graphene, and a vacuum layer of at least 20 Å. All atoms except the bottom substrate layer were fully relaxed until the net force on each relaxed atom was less than 0.01 eV/Å. Various sites were calculated for the adsorption of Hf atoms on graphene/Ir(111) and the creation of carbon vacancies in Hf/graphene/Ir(111). Both fcc and hcp regions were taken into account for the Hf penetration calculations. The pathways for the penetration and interfacial diffusion of Hf atoms were simulated using the climbing-image nudged elastic band (CI-NEB) method.[39,40]

3. Results and discussion

According to the mechanism for heteroatoms' intercalation in epitaxial defect-free graphene proposed by Li *et al.*,[30] the whole intercalation process consists of the following four key stages: (i) adsorption of heteroatoms on graphene/metal and creation of carbon vacancies, (ii) penetration of heteroatoms into graphene/metal interface via carbon vacancies, (iii) self-repairing of graphene lattice, (iv) migration of heteroatoms at the interface and growth of an intercalated layer. Based on this mechanism, we first investigate the possible adsorption sites of Hf atoms on graphene/Ir(111). For graphene/Ir(111), the optimized atomic configuration is shown in Figs. 1(a) and 1(b). The graphene is slightly corrugated due to the weak interaction between graphene and Ir(111). The interface spacing is 3.19 Å and the graphene ripple size is 0.57 Å, in agreement with the calculated results using PBE-D3 (see Figs. S1(a) and S1(b)). Four high-symmetric regions, namely fcc, hcp, atop and bridge, are marked in Fig. 1(a). We calculate the electronic structures of graphene/Ir(111) to check the strength of orbital hybridization between Hf atoms and carbon atoms of the four high-symmetric regions, whereby the possible adsorption sites of Hf atoms can be determined. Figure 1(c) shows the projected density of states (PDOS) on p_z orbitals of C_a and C_b atoms, which denote the two types of carbon atoms contained in graphene lattice. We find that the C_a atoms in hcp region have the highest PDOS intensity near the Fermi level, implying that they are most active to interact with the Hf adatoms. The electronic structures of graphene/Ir(111) calculated using PBE-D3 have similar results (see Fig. S1(c)).

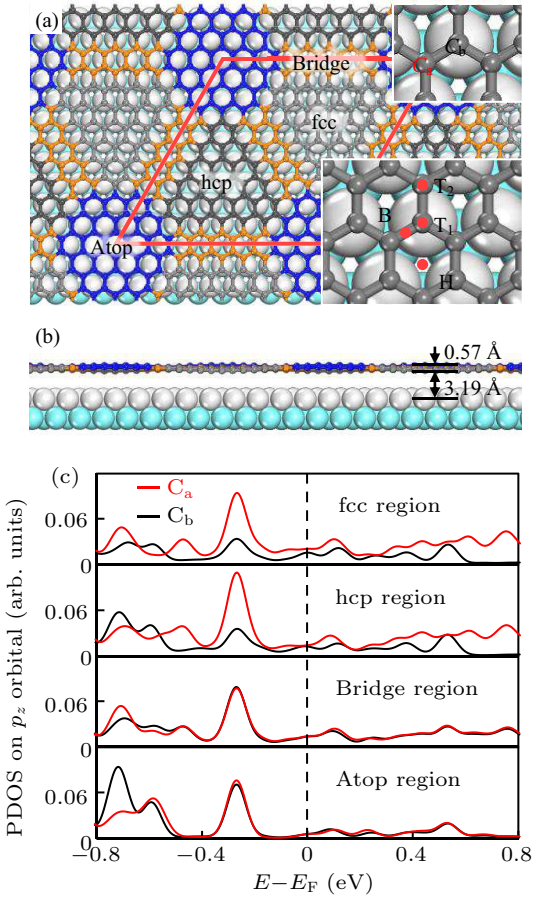


Fig. 1. Configuration and projected density of states of graphene on Ir(111). (a) and (b) Top and side views of the configuration of graphene/Ir(111), respectively. The carbon atoms in the fcc, hcp, bridge and atop regions are marked in grey, black, orange and blue, respectively. Two types of carbon atoms are contained in a unit cell of graphene lattice, as labelled by C_a and C_b in the upper-right inset of (a). The lower-right inset of (a) shows the typical adsorption sites on graphene/Ir(111) with red dots. H, B, and T denote hollow, bridge, and top adsorption sites, respectively. The interface spacing and graphene corrugation in graphene/Ir(111) are illustrated in (b). (c) The projected density of states on p_z orbitals of C_a and C_b atoms in different regions of graphene/Ir(111).

The adsorption sites of Hf atoms on graphene/Ir(111) are further checked by calculating the adsorption energies be-

tween Hf atoms and graphene/Ir(111). The definition of adsorption sites is illustrated in the lower-right inset of Fig. 1(a). Among them, T_1 and T_2 denote the top of C_a or C_b atoms, B denotes the bridge of two nearest carbon atoms, and H denotes the hollow of a hexagonal benzene ring. The adsorption energy E_{ads} is defined as follows:

$$E_{ads} = E_{Hf/graphene/Ir} - E_{graphene/Ir} - E_{Hf},$$

where $E_{Hf/graphene/Ir}$ is the total energy of a Hf adatom on graphene/Ir(111), $E_{graphene/Ir}$ is the total energy of graphene/Ir(111), and E_{Hf} is the energy of a single Hf atom. The adsorption energies at different adsorption sites are summarized in Table 1. We find that for each high-symmetric region, the most stable adsorption site for Hf atoms is the hollow site. Such results can be attributed to the electronic structure of Hf atoms, which has a valence shell configuration of $5d^26s^2$ with four unpaired electrons. The maximum number of Hf–C bonds can be formed when Hf atoms are absorbed at hollow sites. Hollow sites in the hcp region are most preferred, which is consistent with the PDOS calculations in Fig. 1(c). However, since the adsorption energy in the fcc region is almost the same as that in the hcp region, the adsorption of Hf atoms in both regions will be taken into account in the subsequent calculations.

Table 1. Adsorption energies of a hafnium atom on different adsorption sites of graphene/Ir(111), in units of eV. For some adsorption sites, the hafnium atom cannot be stably adsorbed and migrate to other sites after structure optimization, which is represented by initial adsorption site → final adsorption site.

	fcc region	hcp region	Bridge region	Atop region
Top site (T_1)	–3.94	–3.91	–2.73	–2.69
Top site (T_2)	$T_2 \rightarrow H$	–2.65	–2.71	–2.70
Hollow site	–4.12	–4.13	–3.01	–2.93
Bridge site	$B \rightarrow T_1$	$B \rightarrow H$	$B \rightarrow H$	$B \rightarrow H$

Then we investigate the formation of a carbon vacancy in Hf/graphene/Ir(111), which is the prerequisite for the penetration of Hf atoms, as schematically shown in Fig. 2(a). We calculate the vacancy formation energies of the carbon vacancies, which can provide the possibility of their formation. The formula used to calculate the vacancy formation energy is given as follows:

$$E_v = E_{Hf/graphene_vac/Ir} + E_{Carbon} - E_{Hf/graphene/Ir},$$

where $E_{Hf/graphene_vac/Ir}$ is the total energy of a Hf adatom on top of defected graphene on Ir(111), E_{Carbon} is the chemical potential of a single carbon atom in free-standing graphene, $E_{Hf/graphene/Ir}$ is the total energy of Hf/graphene/Ir(111). Considering that Hf atoms were absorbed at the hollow sites in graphene, we locate the vacancy at various carbon sites of the hexagonal ring and calculate the corresponding vacancy formation energies (see Fig. S2 and Table S1). The vacancy formation energies in the fcc and hcp regions are 0.50 eV and 0.30 eV, respectively. These vacancy sites were chosen for the following penetration barrier calculations. It has been reported that for graphene/metal systems, the adsorption of heteroatoms will facilitate the formation of carbon vacancies in graphene.[30] In the case of Si/graphene/Ru, the vacancy formation energy in graphene is as low as 0.23 eV.[30] Our calculated values are comparable to those of Si/graphene/Ru, indicating the possibility of creating carbon vacancies in Hf/graphene/Ir(111).

In the presence of a carbon vacancy in graphene, the penetration of Hf atoms from the surface to the interface can be achievable. We then investigate the penetration process of Hf atoms and the corresponding energy barriers. Figure 2(a) shows the intercalation path of a Hf atom in graphene/Ir(111). From the middle panel, we find that the Hf atom passes through the vacancy with neighboring carbon atoms on its one side being pressed down and those on the other side being lifted up. We speculate that this penetration behavior is induced by the large atomic size of Hf, since the Hf atom enlarges the vacancy hole before passing through. The corresponding energy barriers of Hf atoms penetration in the fcc and hcp regions of graphene/Ir(111) are shown in Figs. 2(d) and 2(e), respectively. The energy barriers are 2.14 eV and 2.38 eV in the fcc and hcp regions, respectively. Both energy barriers are larger than that of Si intercalation at graphene/Ru(0001) interface[30] because of the large size of Hf atoms. For comparison, we also calculate the Hf atoms intercalation in free-standing graphene, as shown in Figs. 2(b) and 2(c). The penetration process of Hf atoms in free-standing graphene is analogous to that in graphene/Ir(111), but the penetration barrier in free-standing graphene is even higher, that is, 5.15 eV, suggesting that this process is unlikely to happen in reality. As reported previously,[30] the penetration barriers of Si atoms in graphene/Ru and free-standing graphene are 0.66 eV and 0.33 eV, respectively, which are smaller than those of Hf atoms. The larger penetration barriers of Hf atoms suggest that the Hf intercalation process will happen at annealing temperatures higher than those of Si intercalation. Moreover, we estimate that even the annealing temperature is increased to 1300 K, the intercalation rate of Hf atoms in graphene/Ir(111) is still 5 to 6 orders of magnitude lower than that of Si atoms in graphene/Ru(0001) with the annealing temperature at around 700 K–900 K (see Fig. S3). As mentioned in previous work,[31] low intercalation rates would induce a longer average penetration time and surface residues. This suggests that in addition to increasing the annealing temperature, the amount of Hf atoms deposited should be reduced, which will help to avoid Hf atoms remaining on the surface due to low intercalation rates. Therefore, due to the highly large penetration barriers, Hf intercalation should be carried out with low deposition doses of Hf atoms and high annealing temperatures.

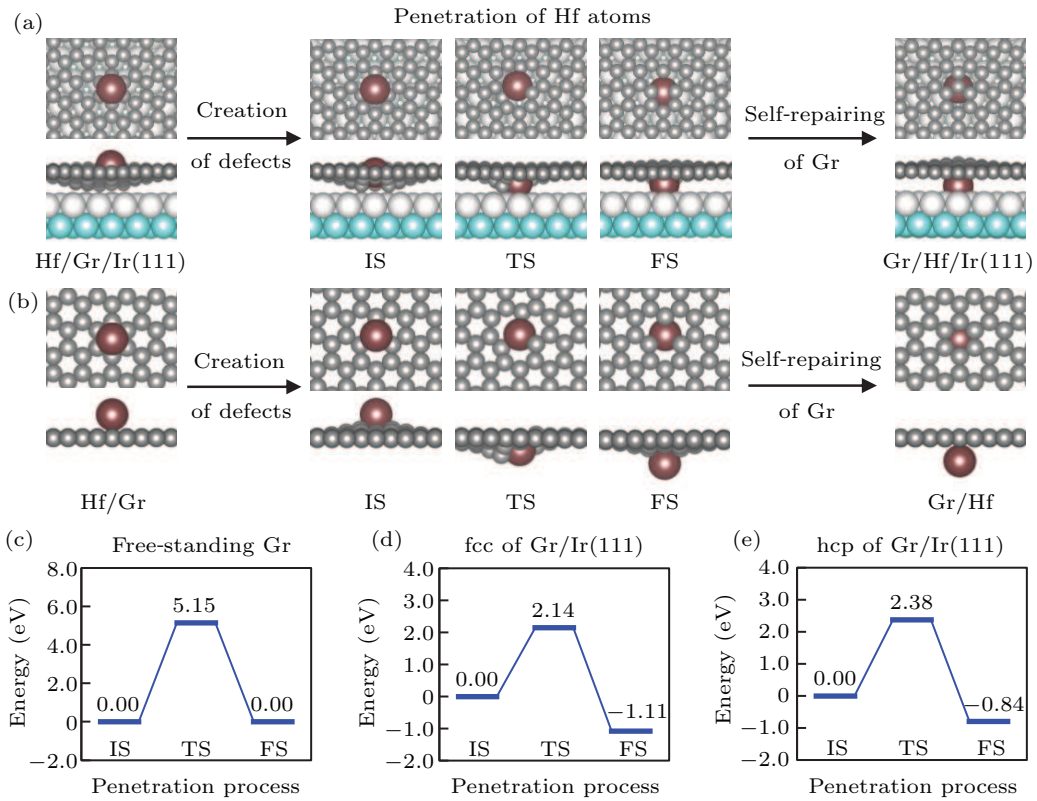


Fig. 2. Configurations of Hf intercalation process and the corresponding energy barriers. (a) and (b) Configurations during the Hf intercalation process for graphene/Ir(111) and free-standing graphene, respectively. The process includes creation of a carbon vacancy, penetration of the Hf atom, and self-repairing of graphene. Gr denotes graphene. IS, TS, and FS denote initial state, transition state, and final state of the penetration process, respectively. In the penetration process, the Hf atom locates at the site of the missing C atom. (c)–(e) Energy barriers of Hf atoms penetrating through the freestanding graphene, the fcc region of graphene/Ir(111), and the hcp region of graphene/Ir(111), respectively.

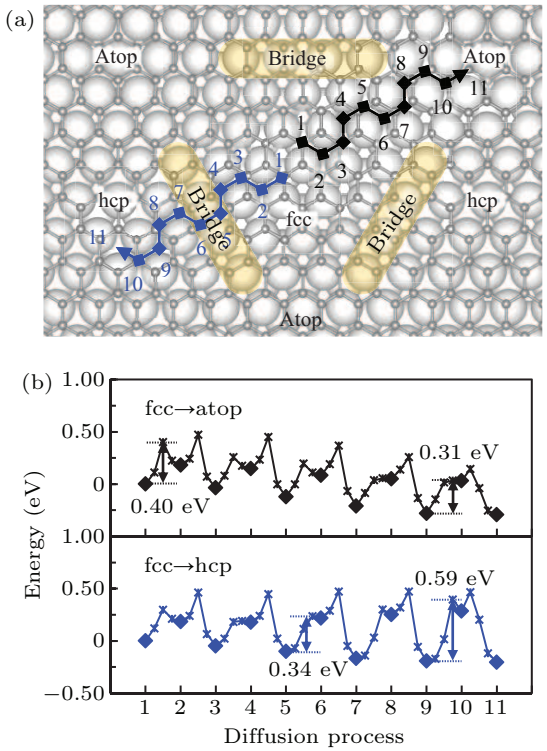


Fig. 3. Hf atoms diffusion at the interface of graphene/Ir(111). (a) Schematic diffusion paths and (b) diffusion barriers of Hf atoms from the fcc region to the atop and hcp regions.

Finally, we investigate the Hf atoms diffusion at the interface of graphene/Ir(111). According to the proposed mechanism, when the penetration of Hf atoms is accomplished, the self-repairing of defected graphene will occur simultaneously,[30] as schematically shown in Fig. 2(a). Then the Hf atoms will diffuse under the graphene to form an interface layer. We calculate the interfacial diffusion barriers to provide the possibility of the formation of the interface layer. We first evaluate the preferable regions for Hf atoms to stay under graphene by calculating the total energies of different graphene/Hf/Ir(111) structures. Table S2 shows that the structure is most stable when Hf atoms are located in the atop region, followed by the hcp region, then the bridge region, and finally the fcc region. By assuming that Hf atoms penetrate in the fcc region, we then simulate two diffusion paths: one is from fcc to atop, corresponding to the diffusion of Hf atoms from the penetration region to the most stable region underneath graphene; the other is from fcc to hcp, which is the subsequent process after the atop region is filled with Hf atoms. The two diffusion paths and their corresponding diffusion barriers are shown in Figs. 3(a) and 3(b), respectively. We find that the interfacial diffusion barriers of Hf atoms are in the range of 0.31–0.59 eV, which are comparable to that of Si atoms (0.5 eV) in graphene/Si/Ru(0001).[30] The small interfacial diffusion barriers suggest that Hf atoms can easily diffuse at the interface of graphene/Ir(111) and form an intercalated layer.

Previous experimental results have shown that a 2×2 superlattice of Hf atoms can be formed at the interface of graphene/Ir(111).[27] Furthermore, the Raman spectra have indicated that the graphene is decoupled from the Ir(111) substrate after Hf intercalation.[27] Therefore, we believe that the intercalated Hf layer weakens the interaction between epitaxial graphene and Ir substrate.

4. Conclusions and perspectives

In summary, we have studied the Hf intercalation between graphene and Ir(111). Due to the large atomic size of Hf, the energy barriers of Hf penetration are large, which will lead to restricted conditions for Hf intercalation experiments. When Hf intercalation is performed based on intact epitaxial graphene, we suggest that it should be carried out with low deposition doses of Hf atoms and high annealing temperatures, which will prevent Hf atoms from aggregating into larger clusters and provide sufficient energy supply for Hf atoms to overcome the large penetration barriers. Otherwise, Hf atoms may be pinned to the surface or get stuck in the created vacancies, which cannot guarantee the clean interface of the fabricated heterostructure and the high quality of graphene. These theoretical results can provide important guidance for the future integration of epitaxial graphene and the high-κ HfO_2 dielectrics.

Acknowledgements

A portion of the research was performed in CAS Key Laboratory of Vacuum Physics. Computational resources were provided by the National Supercomputing Center in Tianjin.

Project supported by the National Natural Science Foundation of China (Grant No. 61888102), the Strategic Priority Research Program of the Chinese Academy of Sciences (Grant No. XDB30000000), and the Fundamental Research Funds for the Central Universities, China.

References

[1] Novoselov K S, Geim A K, Morozov S V, Jiang D, Zhang Y, Dubonos S V, Grigorieva I V and Firsov A A 2004 *Science* **306** 666
[2] Geim A K and Novoselov K S 2007 *Nat. Mater.* **6** 183
[3] Castro Neto A H, Guinea F, Peres N M R, Novoselov K S and Geim A K 2009 *Rev. Mod. Phys.* **81** 109
[4] Pan Y, Zhang H G, Shi D X, Sun J T, Du S X, Liu F and Gao H J 2009 *Adv. Mater.* **21** 2777
[5] N'Diaye A T, Coraux J, Plasa T N, Busse C and Michely T 2008 *New J. Phys.* **10** 16
[6] Gao L, Guest J R and Guisinger N P 2010 *Nano Lett.* **10** 3512
[7] Gao M, Pan Y, Zhang C D, Hu H, Yang R, Lu H L, Cai J M, Du S X, Liu F and Gao H J 2010 *Appl. Phys. Lett.* **96** 053109
[8] Gao M, Pan Y, Huang L, Hu H, Zhang L Z, Guo H M, Du S X and Gao H J 2011 *Appl. Phys. Lett.* **98** 033101
[9] Meng L, Wu R T, Zhang L Z, Li L F, Du S X, Wang Y L and Gao H J 2012 *J. Phys.: Condens. Matter* **24** 314214
[10] Kang J, Shin D, Bae S and Hong B H 2012 *Nanoscale* **4** 5527
[11] Chen Y, Gong X L and Gai J G 2016 *Adv. Sci.* **3** 1500343
[12] Li X S, Zhu Y W, Cai W W, Borysiak M, Han B Y, Chen D, Piner R D, Colombo L and Ruoff R S 2009 *Nano Lett.* **9** 4359
[13] Huang L, Pan Y, Pan L D, Gao M, Xu W Y, Que Y D, Zhou H T, Wang Y L, Du S X and Gao H J 2011 *Appl. Phys. Lett.* **99** 163107
[14] Fei X M, Zhang L Z, Xiao W D, Chen H, Que Y D, Liu L W, Yang K, Du S X and Gao H J 2015 *J. Phys. Chem. C* **119** 9839
[15] Petrovic M, Rakic I S, Runte S, Busse C, Sadowski J T, Lazic P, Pletikosic I, Pan Z H, Milun M, Pervan P, Atodiresei N, Brako R, Sokcevic D, Valla T, Michely T and Kralj M 2013 *Nat. Commun.* **4** 2772
[16] Granas E, Andersen M, Arman M A, Gerber T, Hammer B, Schnadt J, Andersen J N, Michely T and Knudsen J 2013 *J. Phys. Chem. C* **117** 16438
[17] Zhang H, Fu Q, Cui Y, Tan D L and Bao X H 2009 *J. Phys. Chem. C* **113** 8296
[18] Mao J H, Huang L, Pan Y, Gao M, He J F, Zhou H T, Guo H M, Tian Y, Zou Q, Zhang L Z, Zhang H G, Wang Y L, Du S X, Zhou X J, Castro Neto A H and Gao H J 2012 *Appl. Phys. Lett.* **100** 093101
[19] Meng L, Wu R T, Zhou H T, Li G, Zhang Y, Li L F, Wang Y L and Gao H J 2012 *Appl. Phys. Lett.* **100** 083101
[20] Que Y D, Zhang Y, Wang Y L, Huang L, Xu W Y, Tao J, Wu L J, Zhu Y M, Kim K, Weinl M, Schreck M, Shen C M, Du S X, Liu Y Q and Gao H J 2015 *Adv. Mater. Interfaces* **2** 1400543
[21] Li G, Zhang L Z, Xu W Y, Pan J B, Song S R, Zhang Y, Zhou H T, Wang Y L, Bao L H, Zhang Y Y, Du S X, Ouyang M, Pantelides S T and Gao H J 2018 *Adv. Mater.* **30** 1804650
[22] Guo H, Wang X Y, Huang L, Jin X, Yang Z Z, Zhou Z, Hu H, Zhang Y Y, Lu H L, Zhang Q H, Shen C M, Lin X, Gu L, Dai Q, Bao L H, Du S X, Hofer W, Pantelides S T and Gao H J 2020 *Nano Lett.* **20** 8584
[23] Lizzit S, Larciprete R, Lacovig P, Dalmiglio M, Orlando F, Baraldi A, Gammelgaard L, Barreto L, Bianchi M, Perkins E and Hofmann P 2012 *Nano Lett.* **12** 4503
[24] Wang X Y, Guo H, Lu J C, Lu H L, Lin X, Shen C M, Bao L H, Du S X and Gao H J 2021 *Chin. Phys. B* **30** 048102
[25] Wang X Y, Guo H, Shi J A, Biao Y, Li Y, Han G Y, Zhang S, Qian K, Zhou W, Lin X, Du S X, Shen C M, Lu H L and Gao H J 2022 *Rare Metals* **41** 304
[26] Robertson J 2006 *Rep. Prog. Phys.* **69** 327
[27] Li L F, Wang Y L, Meng L, Wu R T and Gao H J 2013 *Appl. Phys. Lett.* **102** 093106
[28] Granas E, Knudsen J, Schroder U A, Gerber T, Busse C, Arman M A, Schulte K, Andersen J N and Michely T 2012 *ACS Nano* **6** 9951
[29] Schroder U A, Granas E, Gerber T, Arman M A, Martinez-Galera A J, Schulte K, Andersen J N, Knudsen J and Michely T 2016 *Carbon* **96** 320
[30] Li G, Zhou H T, Pan L D, Zhang Y, Huang L, Xu W Y, Du S X, Ouyang M, Ferrari A C and Gao H J 2015 *J. Am. Chem. Soc.* **137** 7099
[31] Cui Y, Gao J F, Jin L, Zhao J J, Tan D L, Fu Q and Bao X H 2012 *Nano Res.* **5** 352
[32] Kresse G and Furthmuller J 1996 *Comput. Mater. Sci.* **6** 15
[33] Kresse G and Furthmuller J 1996 *Phys. Rev. B* **54** 11169
[34] Blochl P E 1994 *Phys. Rev. B* **50** 17953
[35] Feibelman P J 2008 *Phys. Rev. B* **77** 165419
[36] Feibelman P J 2009 *Phys. Rev. B* **80** 085412
[37] Zhang L Z, Du S X, Sun J T, Huang L, Meng L, Xu W Y, Pan L D, Pan Y, Wang Y L, Hofer W A and Gao H J 2014 *Adv. Mater. Interfaces* **1** 1300104
[38] Grimme S 2006 *J. Comput. Chem.* **27** 1787
[39] Henkelman G and Jonsson H 2000 *J. Chem. Phys.* **113** 9978
[40] Henkelman G, Uberuaga B P and Jonsson H 2000 *J. Chem. Phys.* **113** 9901